Multicomponent Adsorption and Chromatography with Uneven Saturation Capacities

Tingyue Gu, Gow-Jen Tsai, and George T. Tsao
School of Chemical Engineering and Laboratory of Renewable Resources Engineering, Purdue University, West Lafayette, IN 47907

In chromatographic separations involving elutes with large differences in the molecular size, the adsorption saturation capacities of the elutes may differ because of the differences in the degree of size exclusion. With uneven saturation capacities, isotherm crossovers may occur, which often results in selectivity reversal. In this work, a new multicomponent isotherm has been developed for this kind of system. The isotherm is an extension of the common multicomponent Langmuir isotherm and introduces no or a very limited number of new parameters for its construction. The isotherm crossover conditions have also been derived. Simulations based on a general rate model using the new isotherm have successfully demonstrated the phenomena of peak reversal and crossover of breakthrough curves.

Introduction

Because of the rapid development of preparative and large-scale chromatography for bioseparations, there has been a demand for adequate mathematical modelings of various chromatographic processes. Unlike analytical liquid chromatography, preparative and large-scale chromatography often involves various mass transfer resistances, and the process is often nonlinear due to volume or concentration overload. For chromatographic separation of large biomolecules (such as proteins) using porous adsorbents, size exclusion becomes significant. In such cases, some large molecules can access neither part of the small macropores in the adsorbent particles nor the entire adsorbent particles at all. This is especially true for chromatographic separations of proteins such as affinity chromatography in which large macromolecules are present. For a multicomponent system involving components with different molecular sizes, the extent of size exclusion is not the same for all the components. This often causes uneven adsorption saturation capacities for the components. The least excluded component tends to have the highest saturation capacity and vice versa.

A study of size exclusion coupled with adsorption is a relatively new topic. In the past, size exclusion chromatography has been used to separate compounds with different molecular sizes. The component with a larger molecular size has less chances to penetrate the macropores of the adsorbent, thus it has a smaller retention time. A size exclusion adsorbent (or gel) should have minimum adsorption ability, since adsorption is often considered an undesirable side effect in size exclusion chromatography. It disrupts the retention sequence determined by molecular size distribution of the components. Ironically, the size exclusion comes as a side effect of nonsize exclusion chromatography, such as affinity and adsorption chromatography.

Uneven saturation capacities caused by size exclusion or other reasons bring serious complications in mathematical modeling, and its research deserves special attention (Ruthven, 1984; Huang and Horvath, 1987; Belew et al., 1987; Huang and Guichon, 1989; Fallah et al., 1990). Multicomponent Langmuir isotherm is a widely used multicomponent isotherm because of its simplicity and applicability. Unfortunately, it violates the Gibbs-Duhem law of thermodynamics (Kemball et al., 1947; Ruthven, 1984).

In this work, a new isotherm equation system has been developed for multicomponent systems with uneven saturation capacities induced either by size exclusion or some chemical reasons. The crossover of the isotherm has been studied using a general rate model with the new isotherm to demonstrate the "peak reversal" phenomenon in multicomponent elution and crossover of breakthrough curves.

Correspondence concerning this article should be addressed to G. T. Tsao.

Theory and Mathematical Models

General multicomponent rate model

The general multicomponent rate model used (Gu et al., 1990) considers axial dispersion, external film mass transfer resistance, and intraparticle diffusion. It assumes a local equilibrium for each component between the pore surface and the stagnant fluid phase in the macropores.

$$-D_{bi}\frac{\partial^2 C_{bi}}{\partial Z^2}+v\frac{\partial C_{bi}}{\partial Z}+\frac{\partial C_{bi}}{\partial t}+\frac{3k_i(1-\epsilon_b)}{\epsilon_b R_p}(C_{bi}-C_{pi,R=R_p})=0 \quad (1)$$

$$(1-\epsilon_p)\frac{\partial C^s_{pi}}{\partial t}+\epsilon_p\frac{\partial C_{pi}}{\partial t}-\epsilon_p D_{pi}\left[\frac{1}{R^2}\frac{\partial}{\partial R}\left(R^2\frac{\partial C_{pi}}{\partial R}\right)\right]=0 \quad (2)$$

with the initial and boundary conditions:

$$t=0,\ C_{bi}=C_{bi}(0,Z),\quad C_{pi}=C_{pi}(0,R,Z) \quad (3,\ 4)$$

$$Z=0,\ \frac{\partial C_{bi}}{\partial Z}=\frac{v}{D_{bi}}[C_{bi}-C_{fi}(t)]\quad Z=L,\ \frac{\partial C_{bi}}{\partial Z}=0 \quad (5,\ 6)$$

$$R=0,\ \frac{\partial C_{pi}}{\partial R}=0\quad R=R_p,\ \frac{\partial C_{pi}}{\partial R}=\frac{k_i}{\epsilon_p D_{pi}}(C_{bi}-C_{pi,R=R_p}) \quad (7,\ 8)$$

The model equations can be transformed into the following dimensionless equations:

$$-\frac{1}{Pe_{Li}}\frac{\partial^2 c_{bi}}{\partial z^2}+\frac{\partial c_{bi}}{\partial z}+\frac{\partial c_{bi}}{\partial \tau}+\xi_i(c_{bi}-c_{pi,r=1})=0 \quad (9)$$

$$\frac{\partial}{\partial \tau}\left[(1-\epsilon_p)c^s_{pi}+\epsilon_p c_{pi}\right]-\eta_i\left[\frac{1}{r^2}\frac{\partial}{\partial r}\left(r^2\frac{\partial c_{pi}}{\partial r}\right)\right]=0 \quad (10)$$

with the initial condition,

$$\tau=0,\quad c_{bi}=c_{bi}(0,z),\quad c_{pi}=c_{pi}(0,r,z) \quad (11,\ 12)$$

and with the boundary condition,

$$z=0,\quad \frac{\partial c_{bi}}{\partial z}=Pe_{Li}\left(c_{bi}-C_{fi}(\tau)/C_{0i}\right). \quad (13)$$

For frontal adsorption,

$$C_{fi}(\tau)/C_{0i}=1.$$

For elution,

$$C_{fi}(\tau)/C_{0i}=\begin{cases}1 & 0\le\tau\le\tau_{\text{imp}}\\ 0 & \text{else}\end{cases}.$$

After the sample introduction (in the form of frontal adsorption):

If component i is displaced,

$$C_{fi}(\tau)/C_{0i}=0$$

If component i is a displacer,

$$C_{fi}(\tau)/C_{0i}=1.$$

$$z=1,\quad \frac{\partial c_{bi}}{\partial z}=0 \quad (14)$$

$$r=0,\quad \frac{\partial c_{pi}}{\partial r}=0\quad r=1,\ \frac{\partial c_{pi}}{\partial r}=Bi_i(c_{bi}-c_{pi,r=1}) \quad (15,\ 16)$$

In Eq. 2, c^s_{pi} is the dimensionless concentration of component i in the solid phase of the particles. It is linked directly to a multicomponent isotherm such as the following commonly used multicomponent Langmuir isotherm.

$$C^s_{pi}=\frac{a_i C_{pi}}{1+\sum_{j=1}^{Ns} b_j C_{pj}}$$

that is,

$$c^s_{pi}=\frac{a_i c_{pi}}{1+\sum_{j=1}^{Ns}(b_j C_{0j})c_{pj}}\ \text{(dimensionless)} \quad (17)$$

Extensions of the general multicomponent rate model

The assumption that there exists a local equilibrium for each component between the stagnant fluid phase inside macropores and the solid phase of the particles may not be satisfied, if the adsorption and desorption rates are not high or the mass transfer rates are relatively much faster. In such cases, isotherm expressions cannot be inserted directly into Eq. 2 to replace c^s_{pi}. Instead, a kinetic expression is often used. The so-called second-order kinetics has been used widely to account for reaction kinetics in the study of affinity chromatography (Chase, 1984a,b; Arnold et al., 1985; 1986a,b; Arve and Liapis, 1987). A general rate model with second-order kinetics was applied to affinity chromatography by Arve and Liapis (1987).

The second-order kinetics assumes the following reversible binding and dissociation reaction.

$$P_i+L \underset{k_{di}}{\overset{k_{ai}}{\rightleftharpoons}} P_iL \quad (18)$$

where P_i is component i in the fluid, and L represents active binding sites or immobilized ligands. In Eq. 17, the binding kinetics is of second-order and the disassociation first-order, as shown by the rate expression below.

$$\frac{\partial C^s_{pi}}{\partial t}=k_{ai}C_{pi}\left(C^{\infty}-\sum_{j=1}^{Ns}C^s_{pj}\right)-k_{di}C^s_{pi} \quad (19)$$

where k_{ai} and k_{di} are the adsorption and desorption rate constants for component i, respectively. The rate constant k_{ai} has

a unit of concentration over time while the rate constant k_{di} has a unit of inverse time.

If the reaction rates are relatively large compared to mass transfer rates, then instant adsorption/desorption equilibrium can be assumed such that both sides of Eq. 19 can be set to zero, which consequently gives the Langmuir isotherms with the equilibrium constant $b_i = k_{ai}/k_{di}$ for each component.

Introducing dimensionless groups $Da_i^a = L(k_{ai}C_{0i})/v$ and $Da_i^d = Lk_{di}/v$ which are defined as the Damkölher numbers (Froment and Bischoff, 1979) for adsorption and desorption, respectively, Eq. 19 can be nondimensionalized as follows.

$$\frac{\partial c_{pi}^s}{\partial \tau} = Da_i^a c_{pi}\left(c^\infty - \sum_{j=1}^{Ns} \frac{C_{0j}}{C_{0i}} c_{pj}^s\right) - Da_i^d c_{pi}^s \qquad (20)$$

If the saturation capacities are the same for all the components at equilibrium, Eq. 20 gives $b_i C_{0i} = Da_i^a/Da_i^d$ and $a_i = C^\infty b_i = c^\infty Da_i^a/Da_i^d$ for the resultant multicomponent Langmuir isotherm. The Damkölher numbers reflect the characteristic reaction times to that of the stoichiometric time. The $b_i = k_{ai}/k_{di}$ values for affinity chromatography are often very large (Chase, 1984b), but it is erroneous to jump to the conclusion based on this alone (that the desorption rate must be much smaller than the adsorption rate since the two processes have different reaction orders), and concentration C_{pi} often is very small at the adsorption term in Eq. 19. It is obvious that the dimensionless Damkölher numbers provide a better comparison in this regard.

Adding the second-order kinetics to the general rate model does not complicate the numerical procedure for its solution since the discretization process is untouched. One only has to add Eq. 20 in the final ODE (ordinary differential equation) system. The final ODE system consists of Eqs. 9, 10 and 20. With the trial values of c_{bi}, c_{pi} and c_{pi}^s in the function subroutine (Gu et al., 1990a) in the FORTRAN code, their derivatives can be evaluated easily from the three ODE expressions.

If Ne elements and N interior collocation points are used for the discretization of Eqs. 9 and 10, there will be $Ns(2Ne+1)(2N+1)$ ODE's in the final ODE system, which are $Ns(2Ne+1)N$ more than in the equilibrium case (Gu, 1990). These extra ODE's come from Eq. 20 at each element node and each interior collocation point for each component.

Addition of size exclusion to the rate model

Several mathematical models have been proposed for size exclusion chromatography (Yau et al., 1979; Kim and Johnson, 1984; Koo and Wankat, 1988), among which the model proposed by Kim and Johnson is particularly helpful for this work. Their model is similar to the general rate model described in this work, except that their model considers size exclusion in single-component systems involving no adsorption. They introduced an "accessible pore volume fraction" to account for the size exclusion effect.

In this work, the symbol ϵ_{pi}^a is used to denote the accessible porosity (i.e., accessible macropore volume fraction) for component i. It implies that for small molecules with no size exclusion effect, $\epsilon_{pi}^a = \epsilon_p$, and for large molecules that are completely excluded from the particles $\epsilon_{pi}^a = 0$. For any medium-sized molecules, $0 < \epsilon_{pi}^a < \epsilon_p$. It is convenient to define a size exclusion factor $0 \le F_i^{ex} \le 1$ such that $\epsilon_{pi}^a = F_i^{ex}\epsilon_p$. To include the size exclusion effect, Eq. 2 should be modified as follows:

$$(1-\epsilon_p)\frac{\partial C_{pi}^s}{\partial t} + \epsilon_{pi}^a \frac{\partial C_{pi}}{\partial t} - \epsilon_{pi}^a D_{pi}\left[\frac{1}{R^2}\frac{\partial}{\partial R}\left(R^2\frac{\partial C_{pi}}{\partial R}\right)\right] = 0 \qquad (21)$$

where the first term $(1-\epsilon_p)(\partial C_{pi}^s/\partial t)$ should be dropped or set to zero, if the component does not bind with the stationary phase. It should be pointed out again that C_{pi}^s in Eq. 21 is based on the unit volume of the solids of the particles excluding the pores measured by the *particle porosity* ϵ_p. For a component that is completely excluded from the particles (i.e., $\epsilon_{pi}^a = 0$) adsorbing only on the outer surface of the particles, Eq. 21 degenerates into the following interfacial mass balance relationship.

$$\frac{\partial C_{pi}^s}{\partial t} = \frac{3k_i}{(1-\epsilon_p)R_p}(C_{bi} - C_{pi,R=R_p}) \qquad (22)$$

This equation can be combined with the bulk phase governing equation (Eq. 1) to give the following equation that is similar to a lumped particle model.

$$-D_{bi}\frac{\partial^2 C_{bi}}{\partial Z^2} + v\frac{\partial C_{bi}}{\partial Z} + \frac{\partial C_{bi}}{\partial t} + \frac{(1-\epsilon_b)(1-\epsilon_p)}{\epsilon_b}\frac{\partial C_{pi}^s}{\partial t} = 0 \qquad (23)$$

where C_{pi}^s either follows the multicomponent isotherms or the expression for reversible binding. If component i does not bind with the stationary phase, $C_{pi}^s = 0$ and the fourth term in Eq. 23 is dropped for that component. A reminder again that the solid-phase concentration of component i, C_{pi}^s, is based on the unit volume of the solid part of the particle excluding pores, i.e., the unit volume of the solid skeleton. The dimensionless form of Eq. 23 is:

$$-\frac{1}{Pe_{Li}}\frac{\partial^2 c_{bi}}{\partial z^2} + \frac{\partial c_{bi}}{\partial z} + \frac{\partial c_{bi}}{\partial \tau} + \frac{(1-\epsilon_b)(1-\epsilon_p)}{\epsilon_b}\frac{\partial c_{pi}^s}{\partial \tau} = 0 \qquad (24)$$

Solution strategy

If no component is totally excluded, addition of the size exclusion effect in the rate models is very simple. One only has to use $\epsilon_{pi}^a D_{pi}$ to replace $\epsilon_p D_{pi}$ in the expression of Bi_i and η_i, and ϵ_{pi}^a in $\epsilon_p c_{pi}$ of Eq. 10.

Mathematically, a singularity occurs in the model equation system when a component (say, component i) is totally excluded from the particles (i.e., $\epsilon_{pi}^a = 0$) if one does not use Eq. 24 to replace Eqs. 9 and 10. It turns out that for numerical calculation, there is no need to worry about this singularity, if ϵ_{pi}^a is given a very small value below that of the tolerance of the ODE solver, which is set to 10^{-5} throughout this work. It is found that this treatment gives the results that have the same values for the first five significant digits as those obtained by using Eq. 24.

One should be aware that the size exclusion of a component affects its saturation capacity in the isotherm. It also affects the effective diffusivity of the component since the tortuosity is related to the accessible porosity. It is clear that using size exclusion in a multicomponent model often leads to the use of uneven saturation capacities for a component with signif-

icant size exclusion and a component without size exclusion. This may cause problems when the multicomponent Langmuir isotherm is used in terms of thermodynamic inconsistency.

Results and Discussion

Multicomponent adsorption systems with uneven saturation capacities

Many multicomponent adsorption systems have different saturation capacities for different components. In such cases, the multicomponent Langmuir isotherm is thermodynamically inconsistent (Ruthven, 1984). Although it can be considered only as an experimental expression used for correlation, it may not be used for extrapolation over a wider concentration range (Ruthven, 1984). In this work, the saturation capacities are based on the unit of molecular counts such as mole, not the weight of solutes per unit volume of particle skeleton. The differences in saturation capacities can be caused by physical or chemical reasons.

Systems with physically-induced uneven saturation capacities

In size exclusion chromatography, adsorption is considered as a side effect that should be avoided. With the rapid growth in the separation of large molecules such as proteins by using various chromatographic methods such as affinity chromatography and ion exchange, the involvement of the size exclusion effect becomes often unavoidable. This is a very important issue that deserves special attention. The adsorption saturation capacities of a multicomponent system with size exclusions cannot be considered equal for components with widely different degrees of size exclusion. The component with a greater degree of size exclusion tends to have a smaller saturation capacity, since some binding sites on the surfaces of macropores are blocked due to size exclusion.

Kinetic and isotherm models

In this work, a novel mathematical treatment is presented for systems with uneven saturation capacities for components with different degrees of size exclusion, which follow the second-order kinetics for binding reactions. It is assumed that one molecule can occupy only one binding site, and its binding or size exclusion does not block the accessibility of other vacant binding sites. It also is a reasonable assumption that one molecule can take only one binding site for affinity chromatography involving low-density immobilized ligands.

Based on these basic assumptions, Eq. 19 can be modified to give the following kinetic expression:

$$\frac{\partial C^s_{pi}}{\partial t} = k_{ai} C_{pi}\left(C_i^{\infty} - \sum_{j=1}^{Ns} \theta_{ij} C^s_{pj}\right) - k_{di} C^s_{pi} \tag{25}$$

where constants $0 < \theta_{ij} \le 1$ are called "discount factors" in this work, which are used to discount the values of C^s_{pj} that belong to the components with a lower degree of size exclusion:

$$\theta_{ij} = \begin{cases} 1 & i=j \text{ or } C_i^{\infty} \ge C_j^{\infty} \\ <1 & C_i^{\infty} < C_j^{\infty} \end{cases} \tag{26}$$

Recalling the earlier definition $F_i^{ex} = \epsilon^a_{pi}/\epsilon_p$, it is clear that for a component with a higher degree of size exclusion, its F_i^{ex} value is smaller and so is its saturation capacity C_i^{∞}. One may reasonably assume that $\theta_{ij} = C_i^{\infty}/C_j^{\infty}$ for those θ_{ij} values that are apparently not equal to unity. If those θ_{ij} values are obtained from experimental correlation, the model then becomes semitheoretical. If adsorption equilibrium is assumed, Eq. 25 becomes:

$$b_i C_{pi}\left(C_i^{\infty} - \sum_{j=1}^{Ns} \theta_{ij} C^s_{pj}\right) - C^s_{pi} = 0 \tag{27}$$

Its rearrangement gives:

$$b_i C_{pi} C_i^{\infty} - \sum_{j=1}^{Ns} b_i C_{pi} \theta_{ij} C^s_{pj} - C^s_{pi} = 0 \tag{28}$$

Equation 28 can be rewritten in the following matrix form.

$$[\mathbf{A}] - [\mathbf{B}][\mathbf{C}^s_p] - [\mathbf{C}^s_p] = 0 \tag{29}$$

which gives the following *extended multicomponent Langmuir isotherm.*

$$[\mathbf{C}^s_p] = ([\mathbf{B}] + [\mathbf{I}])^{-1}[\mathbf{A}] \tag{30}$$

where

$$\mathbf{A}_i = b_i C_{pi} C_i^{\infty},\ \mathbf{B}_{ij} = b_i C_{pi}\theta_{ij}, \text{ and } \mathbf{I}_{ij} = \begin{cases} 1 & i=j \\ 0 & \text{else} \end{cases}$$

For a binary system in which component 1 has a higher degree of size exclusion than component 2, one obtains $\theta_{11} = \theta_{22} = \theta_{21} = 1$ and $\theta_{12} < 1$. The extended binary Langmuir isotherm becomes:

$$C^s_{p1} = \frac{b_1 C_{p1}[(1 + b_2 C_{p2}) C_1^{\infty} - \theta_{12} b_2 C_{p2} C_2^{\infty}]}{1 + b_1 C_{p1} + b_2 C_{p2} + (1 - \theta_{12}) b_1 C_{p1} b_2 C_{p2}} \tag{31}$$

$$C^s_{p2} = \frac{b_2 C_{p2}[(1 + b_1 C_{p1}) C_2^{\infty} - b_1 C_{p1} C_1^{\infty}]}{1 + b_1 C_{p1} + b_2 C_{p2} + (1 - \theta_{12}) b_1 C_{p1} b_2 C_{p2}} \tag{32}$$

It is obvious that the above two isotherm expressions reduce to the common Langmuir isotherm expressions if $C_1^{\infty} = C_2^{\infty}$ and $\theta_{12} = 1$. The extended binary Langmuir isotherm has only one more extra constant θ_{12} apart from $C_1^{\infty} = C_2^{\infty}$ than the common Langmuir isotherm, and θ_{12} may often be reasonably set to $C_1^{\infty}/C_2^{\infty}$.

The extended multicomponent isotherm can also be applied to some adsorption systems with uneven saturation capacities which are not induced by size exclusion.

Systems with chemically-induced, uneven saturation capacities

In some multicomponent systems, uneven saturation capacities do not arise from different degrees of size exclusion, but they are induced by an adsorption mechanism at the molecular level. For example, suppose the binding sites (or ligands)

of a binary system are a racemic mixture, which makes no difference to component 2, but only part of which is active and usable for component 1. Then, component 1 has a lower saturation capacity than component 2. The mathematical treatment for such a system is the same as that for systems with uneven saturation capacities that are induced by size exclusion. The discount factor θ_{12} may also be reasonably set to the ratio $C_1^{\infty}/C_2^{\infty}$. For systems with more than two components, the determination of θ_{ij} values may not be that simple.

Isotherm crossover

With uneven saturation capacities, isotherm "crossover" may occur. This happens when a component with a smaller saturation capacity has a larger adsorption equilibrium concentration. In this work, the isotherm concentration crossover point C_p^c is defined as the concentration in the stagnant fluid inside macropores for a pair of components, at which their concentrations in the solid phase (C_{pi}^s) are the same.

The concentration crossover point for the binary isotherms (Eqs. 31 and 32) can be derived by subtracting the two isotherm expressions and setting $C_{p1}=C_{p2}=C_p^c$.

$$C_{p1}^s - C_{p2}^s = \frac{(b_1C_1^{\infty} - b_2C_2^{\infty})C_p^c + b_1b_2[2C_1^{\infty} - (1+\theta_{12})C_2^{\infty}](C_p^c)^2}{1 + b_1C_p^c + b_2C_p^c + (1-\theta_{12})b_1C_p^cb_2C_p^c} \quad (33)$$

Making the lefthand side of Eq. 33 zero, one obtains:

$$(b_1C_1^{\infty} - b_2C_2^{\infty})C_p^c + b_1b_2[2C_1^{\infty} - (1+\theta_{12})C_2^{\infty}] = 0 \quad (34)$$

which gives a nontrivial solution

$$C_p^c = \frac{b_1C_1^{\infty} - b_2C_2^{\infty}}{b_1b_2[(1+\theta_{12})C_2^{\infty} - 2C_1^{\infty}]} \quad (35)$$

If $\theta_{12}=C_1^{\infty}/C_2^{\infty}$,

$$C_p^c = \frac{b_1C_1^{\infty} - b_2C_2^{\infty}}{b_1b_2(C_2^{\infty} - C_1^{\infty})} \quad (36)$$

The denominator of Eq. 36 is positive since $C_2^{\infty} > C_1^{\infty}$. Thus, the binary isotherm has a crossover point if, and only if, the crossover concentration has a positive value, which requires

$$b_1C_1^{\infty} > b_2C_2^{\infty} \text{ or } \frac{b_1}{b_2} > \frac{C_2^{\infty}}{C_1^{\infty}} \quad (37)$$

Isotherm concentration crossover often signals a selectivity change. The selectivity crossover point in this work is defined as the critical concentration $C_p^c = C_{p1}$ and C_{p2}, with which the relative selectivity of the two components,

$$\text{Relative Selectivity} = \frac{\partial C_{p1}^s/\partial C_{p1}}{\partial C_{p2}^s/\partial C_{p2}}, \quad (38)$$

is unity. The selectivity crossover point can be found by following an approach similar to that for the concentration crossover point. Setting the lefthand side of Eq. 38 to unity yields:

$$\partial C_{p1}^s/\partial C_{p1} - \partial C_{p2}^s/\partial C_{p2} = 0 \quad (39)$$

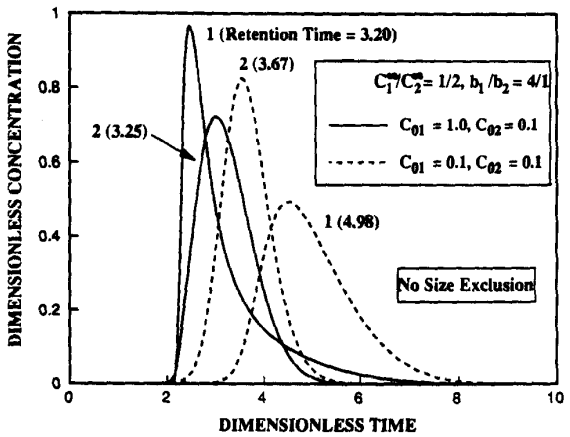

Figure 1. Peak reversal due to increased component 1 concentration.

from which the following critical selectivity crossover concentration can be easily obtained with $C_{p1}=C_{p2}=C_p^c$ and $\theta_{12}=C_1^{\infty}/C_2^{\infty}$:

$$C_p^c = -\frac{1}{b_1} + \frac{1}{b_1}\sqrt{\frac{C_1^{\infty}(b_1-b_2)}{b_2(C_2^{\infty}-C_1^{\infty})}} \quad (40)$$

In Eq. 40 for $C_p^c > 0$, the following equation must be satisfied:

$$\sqrt{\frac{C_1^{\infty}(b_1-b_2)}{b_2(C_2^{\infty}-C_1^{\infty})}} > 1 \quad (41)$$

which readily reduces to Eq. 37. Thus, both concentration crossover and selectivity crossover need to satisfy Eq. 37.

It has been known that selectivity depends on the concentration range, and selectivity reversal may occur in the operational concentration range (Antia and Horvath, 1989). A selectivity reversal may cause the reversal of the sequence of elution peaks since the migration speed of a component is determined primarily by its $\partial C_{pi}^s/\partial C_{pi}$ value (Helfferich and Klein, 1970). Peak reversal in elution usually happens in volume overload cases, if the feed concentration is very high.

Figure 1 shows two binary elution cases, in which component

Table 1. Parameter Values Used for Simulation*

Figure	Species	Physical Parameters Pe_{Li}	η_i	Bi_i	a_i	$b_i \times C_{0i}$	Numerical Parameters Ne	N
1–4	1	300	4	20	4	4×	12–22	2
	2	300	4	20	2	1×		
5	1	300	1	40	4	4×	8	2
	2	300	1	40	2	1×		
6	1	300	1	20	4	4×	8	2
	2	300	1	20	1	0.5×		
7	1	300	1	20	4	4×	10	2
	2	300	4	20	1	0.5×		

*In all cases, $\epsilon_b = 0.4$, $\epsilon_p = 0.4$. For all elution cases, sample sizes are: $\tau_{inp} = 1.0$, except for Figure 4 in which $\tau_{inp} = 0.05$. The error tolerance of the ODE solver is tol = 10^{-5}. Double precision is used in the Fortran code.

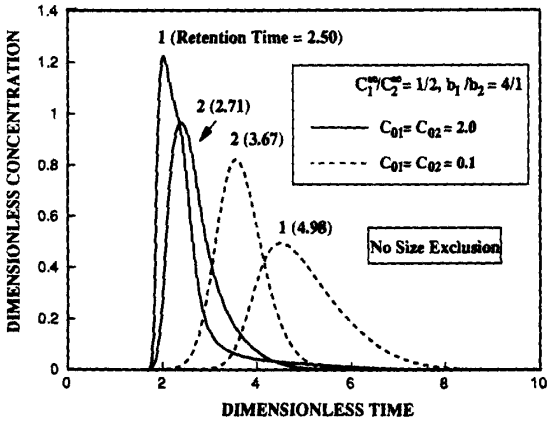

Figure 2. Peak reversal in binary elution without size exclusion.

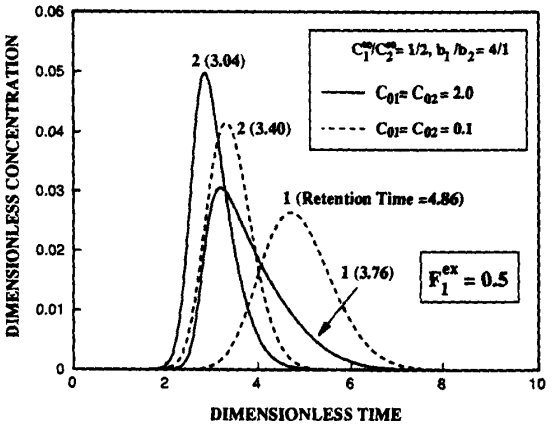

Figure 4. No peak reversal due to small sample size.

1 has a smaller saturation capacity and a higher adsorption equilibrium constant than component 2. Parameter values used for simulation are listed in Table 1. The dashed lines show that component 2 has a smaller retention time than component 1 when the feed concentration of component 1 is low, while the solid lines show that component 2 has a higher retention time when the feed concentration of component 1 is increased tenfold. It is interesting to note that in Figure 1 (solid lines) the tail end of the component 1 peak is behind that of the component 2 peak. Apparently, at low concentrations component 1 has a higher affinity than component 2.

Figure 2 has the same conditions as Figure 1, except that in the solid line case the concentrations of components 1 and 2 are both 2.0 in Figure 2. The peak reversal phenomenon is also present in Figure 2. If the uneven saturation capacities are not chemically-induced, but by size exclusion, peak reversal still can be present. Figure 3 clearly shows such a case in which component 1 has a size exclusion factor of $F_1^{ex} = 0.5$.

In Figures 1-3, the sample size is quite large ($\tau_{imp} = 1.0$) such that a sample is not diluted too much during migration inside the column. Otherwise, the dilution of the sample will quickly move the general working concentration range in the isotherm from that over the isotherm crossover point to below the point. In such a case, peak reversal may not occur at all. Figure 4 has the same conditions as Figure 3, except that in Figure 4 the sample size is much smaller ($\tau_{imp} = 0.05$). There is no peak reversal in Figure 4 (solid lines) because the concentrations of the two sample components are below the isotherm crossover point most of the time during their migration inside the column. Their concentrations are quickly diluted in the initial stage of the migration because of the small sample size.

The selectivity reversal is also very interesting in frontal adsorption. The solid lines in Figure 5 show that the breakthrough curves cross over each other when the feed concentrations are high. Figure 6 (with size exclusion) also shows a crossover of breakthrough curves (solid lines). It should be pointed out that a crossover of breakthrough curves depends on not only the isotherm characteristics and feed concentration, but also on mass transfer conditions. Figure 7 has the same conditions as Figure 6, except that $\eta_2 = 4$ (for component 2) in Figure 7, instead of $\eta_2 = 1$ in Figure 6. There is a reversal of sequence of breakthrough curves when the feed concentrations are increased, but there is no crossover of the two curves. The absence of a crossover of the two breakthrough curves is

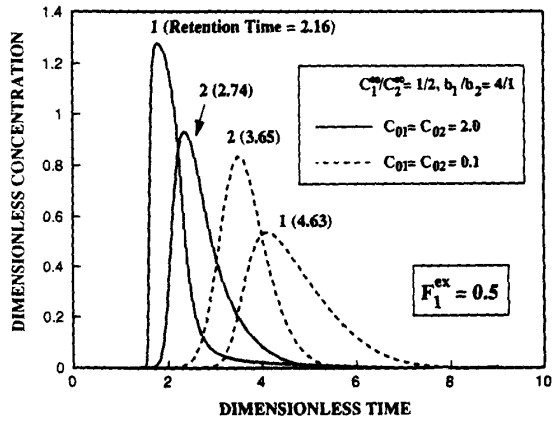

Figure 3. Peak reversal with size exclusion.

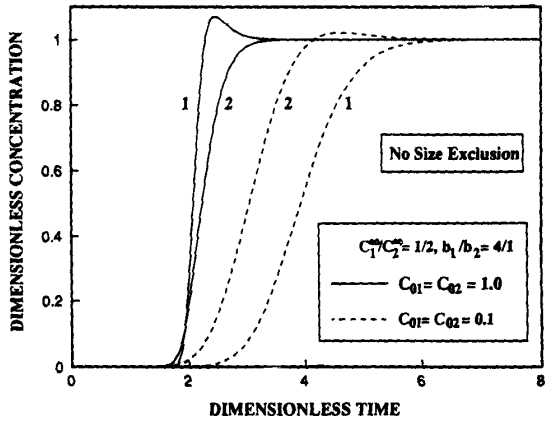

Figure 5. Crossover of breakthrough curves (no size exclusion).

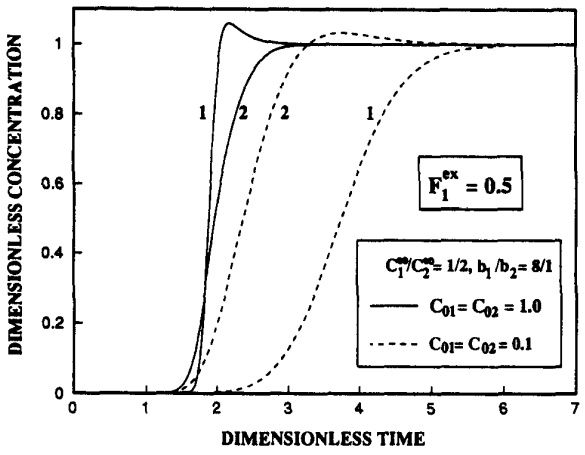

Figure 6. Crossover of breakthrough curves (with size exclusion).

apparently due to the change of the relative positions of the concentration fronts of the two components arising from the change in mass transfer conditions for component 2.

A detailed treatment of peak reversal due to isotherm selectivity crossover is considerably more difficult and involves complicated debate. Peak reversal is not necessarily the consequence of selectivity reversal, although selectivity reversal facilitates the peak reversal phenomenon. In this work, the extended binary Langmuir isotherm successfully demonstrated the peak reversal phenomenon without extreme differences between the feed concentrations and adsorption equilibrium values of the two components. The extended isotherm also serves as a valuable isotherm model for experimental correlation of isotherm data showing uneven saturation capacities. A similar approach can be applied readily to common stoichiometric ion-exchange systems.

Conclusions

In this work, a new isotherm has been proposed for multicomponent systems with uneven saturation capacities induced either by size exclusion or by racemic discrimination of the active sites toward the solutes. The mathematical criteria for isotherm crossover in terms of concentration and selectivity have been derived. A general rate model that considers various mass transfer effects and the new isotherm has been used to demonstrate the phenomena of peak reversals in elution and crossovers of breakthrough curves.

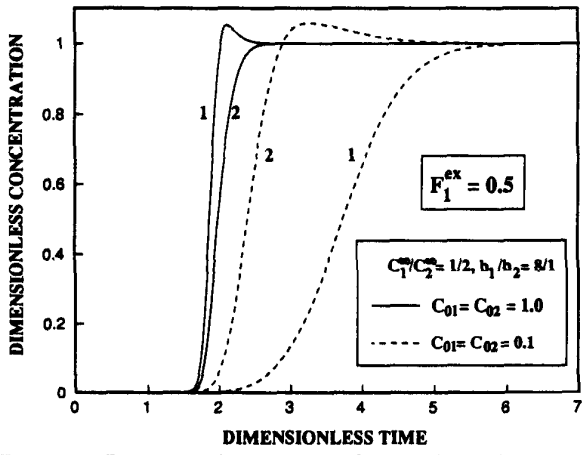

Figure 7. Reversal of sequence of breakthrough curves without their crossover.

Acknowledgment

The authors thank National Science Foundation Grant EET-8613167A2 for support of this research.

Notation

a_i = constant in Langmuir isotherm for component i, $b_iC_i^{\infty}$
b_i = adsorption equilibrium constant for component i, k_{ai}/k_{di}
Bi_i = Biot number of mass transfer for component i, $k_iR_p/(\epsilon_pD_{pi})$
C_{bi} = bulk phase concentration of component i
C_{fi} = feed concentration profile of component i, a time-dependent variable
C_{0i} = concentration used for nondimensionalization, $\max\{C_{fi}(t)\}$,
C_{pi} = concentration of component i in the stagnant fluid phase inside particle macropores
C_p^c = critical concentration for concentration crossover in a binary isotherm
C_{pi}^s = concentration of component i in the solid phase of particle (based on unit volume of particle skeleton)
C_i^{∞} = adsorption saturation capacity for component i (based on unit volume of particle skeleton)
c_{bi} = C_{bi}/C_{0i}
c_{pi} = C_{pi}/C_{0i}
c_{pi}^s = C_{pi}^s/C_{0i}
c_i^{∞} = C_i^{∞}/C_{0i}
D_{bi} = axial or radial dispersion coefficient of component i
D_{pi} = effective diffusivity of component i, porosity not included
Da_i^a = Damkölher number for adsorption
Da_i^d = Damkölher number for desorption, Lk_{di}/v $L(k_{ai}C_{0i})/v$
k_i = film mass transfer coefficient of component i
k_{ai} = adsorption rate constant for component i
k_{di} = desorption rate constant for component i
L = column length
N = number of interior collocation points
Ne = number of quadratic elements
Ns = number of components
Pe_{Li} = Peclet number of axial dispersion for component i, vL/D_{bi}
R = radial coordinate for particle
R_p = particle radius
r = R/R_p
t = time
v = interstitial velocity
Z = axial coordinate
z = Z/L

Greek letters

ϵ_b = bed void volume fraction
ϵ_p = particle porosity
η_i = dimensionless constant, $\epsilon_pD_{pi}L/(R_p^2v)$
ξ_i = dimensionless constant for component i, $3Bi_i\eta_i(1-\epsilon_b)/\epsilon_b$
τ = dimensionless time, vt/L
τ_{imp} = dimensionless time duration for a rectangular pulse of the sample
θ_{ij} = discount factors for extended multicomponent Langmuir isotherm

Literature Cited

Antia, F. D., and C. Horvath, "Operational Modes of Chromatographic Separation Processes," *Ber. Bunsenges. Phys. Chem.*, **93**, 961 (1989).

Arnold, F. H., H. W. Blanch, and C. R. Wilke, "Analysis of Affinity

Separations: I. Predicting the Performance of Affinity Adsorbers," *J. Chromatogr.*, **30**, B9 (1985).
Arnold, F. H., S. A. Schofield, and H. W. Blanch, "Analytical Affinity Chromatography: I. Local Equilibrium Theory and the Measurement of Association and Inhibition Constants," *J. Chromatogr.*, **355**, 1 (1986a).
Arnold, F. H., S. A. Schofield, and H. W. Blanch, "Analytical Affinity Chromatography: II. Rate Theory and the Measurement of Biological Binding Kinetics," *J. Chromatogr.*, **355**, 13 (1986b).
Arve, B. H., and A. I. Liapis, "Modeling and Analysis of Elution Stage of Biospecific Adsorption in Fixed Beds," *Biotech. & Bioeng.*, **30**, 638 (1987).
Belew, M., T.-T. Yip, L. Andersson, and J. Porath, "Quantitation of Adsorption Capacity, Adsorption Isotherms and Equilibrium Constants by Frontal Analysis," *J. Chromatogr.*, **403**, 197 (1987).
Chase, H. A., "Affinity Separations Utilizing Immobilized Monoclonal Antibodies—a New Tool for the Biochemical Engineer," *Chem. Eng. Sci.*, **39**, 1099 (1984a).
Chase, H. A., "Prediction of the Performance of Preparative Affinity Chromatography," *J. Chromatogr.*, **279**, 179 (1984b).
Fallah, M. Z. E., S. Golshan-Shirazi, and G. Guichon, "Theoretical Study of the Effect of a Difference in Column Saturation Capacities for the Two Components of a Binary Mixture on Their Elution Band Profiles and Separation in Nonlinear Chromatography," *J. Chromatogr.*, **511**, 1 (1990).
Froment, G. F., and K. B. Bischoff, *Chemical Reactor Analysis and Design*, Wiley, New York, **529**, 530 (1979).
Gu, T., G.-J. Tsai, and G. T. Tsao, "New Approach to a General Nonlinear Multicomponent Chromatography Model," *AIChE J.*, **36**, 781 (1990).
Gu, T., "Inclusion Chromatography Using Cyclodextrin-Containing Resins and Studies of Nonlinear Chromatographic Theories," PhD Thesis, Purdue Univ., W. Lafayette, IN (Aug., 1990).
Helfferich, F., and G. Klein, *Multicomponent Chromatography—Theory of Interference*, p. 41, Marcel Dekker, New York (1970).
Huang, J.-X., and Cs. Horvath, "Adsorption Isotherms on High-Performance Liquid Chromatographic Sorbents," *J. Chromatogr.*, **406**, 275 (1987).
Huang, J.-X., and G. Guichon, "Competitive Adsorption Behavior in HPLC: cis- and trans-Androsterone on Silica," *J. Colloid and Interface Sci.*, **128**, 577 (1989).
Kemball, C., E. K. Rideal, and E. A. Guggenheim, "Thermodynamics of Monolayers," *Trans. Farad. Soc.*, **44**, 948 (1948).
Kim, D. H., and A. F. Johnson, "Computer Model for Gel Permeation Chromatography of Polymers," T. Provder, ed., *ACS Symp. Ser.*, No. 245, 25 (1984).
Koo, Y.-M., and P. C. Wankat, "Modeling of Size Exclusion Parametric Pumping," *Sep. Sci. Tech.*, **23**, 413 (1988).
Ruthven, D. M., *Principles of Adsorption and Adsorption Processes*, p. 106, Wiley, New York (1984).
Yau, W. W., J. J. Kirkland, and D. D. Bly, *Modern Size-Exclusion Liquid Chromatography*, pp. 31, 57, Wiley, New York (1979).

Manuscript received Nov. 27, 1990, and revision received July 19, 1991.